

RESEARCH PAPER

Postprandial fatty acid uptake and adipocyte remodeling in angiotensin type 2 receptor-deficient mice fed a high-fat/high-fructose diet

Christophe Noll^a, Sébastien M. Labbé^{a,b}, Sandra Pinard^a, Michael Shum^a, Lyne Bilodeau^a, Lucie Chouinard^a, Serge Phoenix^{a,c}, Roger Lecomte^b, André C. Carpentier^a, and Nicole Gallo-Payet^a

^aDepartment of Medicine, Division of Endocrinology, Faculty of Medicine and Health Sciences, Université de Sherbrooke, Sherbrooke, Québec, Canada; ^bThe Québec Heart and Lung Institute Research Center, Université Laval, Québec, Canada; ^cSherbrooke Molecular Imaging Center of CRCHUS and Department of Nuclear Medicine and Radiobiology, Faculty of Medicine and Health Sciences, Université de Sherbrooke, Sherbrooke, Québec, Canada

ABSTRACT

The role of the angiotensin type-2 receptor in adipose physiology remains controversial. The aim of the present study was to demonstrate whether genetic angiotensin type-2 receptor-deficiency prevents or worsens metabolic and adipose tissue morphometric changes observed following a 6-week high-fat/high-fructose diet with injection of a small dose of streptozotocin. We compared tissue uptake of nonesterified fatty acid and dietary fatty acid in wild-type and angiotensin type-2 receptor-deficient mice by using the radiotracer 14(R,S)-[¹⁸F]-fluoro-6-thia-heptadecanoic acid in mice fed a standard or high-fat diet. Postprandial fatty acid uptake in the heart, liver, skeletal muscle, kidney and adipose tissue was increased in wild-type mice after a high-fat diet and in angiotensin type-2 receptor-deficient mice on both standard and high-fat diets. Compared to the wild-type mice, angiotensin type-2 receptor-deficient mice had a lower body weight, an increase in fasting blood glucose and a decrease in plasma insulin and leptin levels. Mice fed a high-fat diet exhibited increased adipocyte size that was prevented by angiotensin type-2 receptor-deficiency. Angiotensin type-2 receptor-deficiency abolished the early hypertrophic adipocyte remodeling induced by a high-fat diet. The small size of adipocytes in the angiotensin type-2 receptor-deficient mice reflects their inability to store lipids and explains the increase in fatty acid uptake in non-adipose tissues. In conclusion, a genetic deletion of the angiotensin type-2 receptor is associated with metabolic dysfunction of white adipose depots, and indicates that adipocyte remodeling occurs before the onset of insulin resistance in the high-fat fed mouse model.

ARTICLE HISTORY

Received 17 September 2015
Revised 20 October 2015
Accepted 27 October 2015

KEYWORDS

Adipose tissue; adipocyte; angiotensin type 2 receptor; high-fat/high-fructose diet; insulin resistance; NEFA

Introduction

Angiotensin II (Ang II), which belongs to the renin-angiotensin system (RAS), mediates its action via 2 major receptors, namely the Ang II type-1 receptor (AT1R) and the type-2 receptor (AT2R). AT2R expression is low in adults, except in a few tissues, such as the heart and steroid-producing glands.¹ Nevertheless, it may be re-expressed when cellular homeostasis is disrupted. More recently, one group found that direct AT2R stimulation using the new selective non-peptide AT2R agonist, compound 21 (C21, also named M24 or M024²), mitigates myocardial ischemic damage in rats by stimulating anti-apoptotic and anti-inflammatory mechanisms.³ However, another group observed no improvement in ventricular remodeling after ischemic damage in mice treated with the C21/M24 AT2R agonist.⁴

These controversies could be extended to the adipose tissue (for review, see¹). In the apolipoprotein E

knockout mouse model of atherosclerosis, AT2R knockout increased adipocyte size and plasma cholesterol and nonesterified fatty acid (NEFA) levels.^{5,6} Conversely, Yvan-Charvet et al.⁷ documented an increased number of small adipocytes in AT2R-deficient mice and concluded that these mice were protected against high fat diet-induced obesity. We have recently developed 2 new models to study the development of T2D. The first is the model of high-fat/high-fructose diet with injection of a small dose of streptozotocin (HFHF-STZ) in Wistar rats that recapitulates the modest hypertriglyceridemia, hyperglycemia, insulin resistance and hypoadiponectinemia observed in patients with recent onset type 2 diabetes.⁸ We therefore applied this model in this study in order to induce a state of pre-diabetes, as previously shown in mice.⁹ It is important to underline, however, that the high-fat and high-fructose diets were not

CONTACT Nicole Gallo-Payet ✉ nicole.gallo-payet@usherbrooke.ca 📧 Division of Endocrinology, Faculty of Medicine and Health Sciences, Université de Sherbrooke, 3001, 12th Avenue North, Sherbrooke, Québec, Canada J1H 5N4.

Color versions of one or more of the figures in this article can be found online at www.tandfonline.com/kadi.

© 2016 Taylor & Francis Group, LLC

administered concurrently in the previously mentioned study and that we used a lower dose of STZ. The second is the recently developed noninvasive method based on intravenous and oral administration of [^{18}F]-FTHA combined with PET for studying NEFA and dietary fatty acid partitioning both in animals and humans.^{8,10} [^{18}F]-FTHA is a long-chain fatty acid analog that has similar cellular uptake to palmitate, but is retained in oxidative as well as nonoxidative cellular pathways.¹¹ Radiotracers display a greater sensitivity to assay fatty acid metabolism than other standard approaches and could provide, when combined with the avalanche photodiode-based micro-PET (μPET), an uptake rate of the tracers in multiple organs. Using μPET methodology, we observed a significant increase in myocardial dietary fatty acid uptake associated with impaired ventricular function,⁸ as recently documented in pre-diabetic subjects.¹⁰ In this rat model of early type 2 diabetes, we also observed a significant shift toward larger adipocytes in visceral and subcutaneous adipose tissue depots,¹² also reminiscent of the adipocyte phenotype observed in patients with pre-diabetes.^{13,14} In our rat model of early type 2 diabetes, a 6-week treatment with the C21/M24 AT2R agonist restored normal adipocyte size distribution in visceral and subcutaneous adipose tissue depots.¹² Similar conclusions were recently published in a model of high-fat diet and obesity in female mice.¹⁵

Hypertrophic remodeling of adipose tissue has been associated with increased adipocyte intracellular lipolytic capacity¹⁶ that may in turn contribute to increase fatty acid flux to lean organs, inducing the development of insulin resistance.^{17,18} Together with the previous observations in C21-treated animals,^{12,15} we questioned the specific role of AT2R in these effects. The aim of the present study was 1) to determine the effect of HFHF-STZ and AT2R genetic deletion on adipocyte remodeling and NEFA and dietary fatty acid metabolism in several tissues by using μPET recordings and 2) to determine whether a genetic deletion of AT2R may

affect these metabolic adaptations early in the development of pre-diabetes.

Results

Effect of AT2R-KO and HFHF-STZ on body weight, biochemical markers and nutritional parameters

As shown in Table 1, weight gain was less significant in AT2R-KO than WT mice on both diets. Heart weight was reduced in WT HFHF-STZ and AT2R-KO mice fed a standard diet. HFHF-STZ treatment induced a decrease in liver weight in both mice strains. No variations were found in skeletal muscle and visceral adipose tissue weights between groups. Leptin levels were also lower in AT2R-KO than WT mice on both diets. While blood glucose was increased in WT HFHF-STZ mice, and in AT2R-KO mice fed with both diets in comparison to WT mice fed a standard diet, no variation was found in glucose tolerance between groups. No difference was observed in plasma NEFA and triglycerides levels between WT and AT2R-KO mice on both diets. Plasma insulin levels were significantly lower in AT2R-KO vs. WT mice fed a standard diet. This difference in insulin levels between AT2R-KO and WT mice was not abolished by HFHF-STZ. As shown in Table 2, WT HFHF-STZ mice consumed less water and food than WT mice fed a standard diet. Even if the HFHF diet is more caloric than the standard diet (6.35 kcal.g^{-1} vs. 4.59 kcal.g^{-1}), WT HFHF-STZ mice consumed fewer calories than WT mice. AT2R-KO mice on both diets consumed less water and food, and fewer calories than WT mice fed a standard diet.

Effect of genetic AT2R deletion and diet on fractional and net plasma NEFA uptake

No significant difference was observed in fractional (Fig. 1A) and net (Fig. 1B) uptake of plasma NEFA in the heart of AT2R-KO vs. WT mice on both diets. Liver

Table 1. Anthropometric and biochemical markers.

	WT SD	WT HFHF-STZ	AT2R-KO SD	AT2R-KO HFHF-STZ
Weight gain (%)	19.4 ± 2.2	21.7 ± 2.5	5.9 ± 1.5 ^a	10.9 ± 2.7 ^b
Blood glucose (mM)	4.2 ± 0.2	6.1 ± 0.5 ^a	7.3 ± 0.5 ^a	8.7 ± 0.7 ^b
Blood glucose AUC _{OGTT} (mM.120 min ⁻¹)	2131 ± 98	2155 ± 84	2029 ± 111	2248 ± 69
Plasma NEFA (μM)	604 ± 87	558 ± 74	708 ± 40	667 ± 70
Plasma triglycerides (μM)	371 ± 33	286 ± 41	301 ± 33	264 ± 46
Plasma insulin (pg.mL ⁻¹)	1993 ± 726	1040 ± 329	309 ± 110 ^a	293 ± 179
Plasma leptin (pg.mL ⁻¹)	1718 ± 394	2731 ± 899	715 ± 207 ^a	1821 ± 737
Heart weight (mg)	158.4 ± 5.6	134.2 ± 2.4 ^a	129.0 ± 5.2 ^a	135.8 ± 7.0
Liver weight (mg)	1233 ± 47	906 ± 43 ^a	1152 ± 76	961 ± 8 ^c
Skeletal muscle (Gastrocnemius) weight (mg)	117.6 ± 10.2	125.5 ± 15.0	105.8 ± 8.4	125.0 ± 9.9
Visceral adipose tissue weight (mg)	903.1 ± 125.6	771.8 ± 162.0	648.2 ± 152.6	878.0 ± 193.2

Values are means ± SE from 9–10 animals per group. Wild-type (WT) and AT2R-knockout-out (KO) mice were fed for 6 weeks either with standard laboratory rodent diet (SD) or with a high-fat/high-fructose with small injection of streptozotocin (HFHF-STZ). Statistical analysis was performed using Mann-Whitney test. a : $P < 0.05$ vs. WT SD ; b : $P < 0.05$ vs. WT HFHF-STZ ; c : $P < 0.05$ vs. AT2R-KO SD.

Table 2. Food and water consumption per day.

	WT SD	WT HFHF-STZ	AT2R-KO SD	AT2R-KO HFHF-STZ
Mean water consumption (mL.day ⁻¹)	6.1 ± 0.2	4.8 ± 0.1 ^a	5.4 ± 0.1 ^a	5.1 ± 0.1
Mean food consumption (g.day ⁻¹)	4.5 ± 0.2	2.3 ± 0.1 ^a	3.7 ± 0.1 ^a	2.3 ± 0.1 ^c
Mean caloric intake (kcal.day ⁻¹)	15.3 ± 0.8	11.2 ± 0.4 ^a	12.7 ± 0.2 ^a	11.6 ± 0.5 ^c

Values are means ± SE from 9–10 animals per group. Wild-type (WT) and AT2R-knockout-out (KO) mice were fed for 6 weeks either with standard laboratory rodent diet (SD) or with a high-fat/high-fructose with small injection of streptozotocin (HFHF-STZ). Statistical analyses were performed using Mann-Whitney test. a: $P < 0.05$ vs. WT SD; b: $P < 0.05$ vs. WT HFHF-STZ; c: $P < 0.05$ vs. AT2R-KO SD.

fractional uptake of plasma NEFA tended to be higher and liver net uptake of plasma NEFA was significantly higher in AT2R-KO vs. WT mice fed a standard diet (Fig. 1C). These differences between AT2R-KO and WT mice were abolished on HFHF-STZ.

Effect of genetic AT2R deletion and HFHF-STZ on dietary fatty acid uptake

Increase in dietary fatty acid uptake was observed in the heart (Fig. 2A, $P < 0.05$), liver (Fig. 2B, $P < 0.02$), skeletal muscles (Fig. 2C, $P < 0.03$), kidney (Fig. 2D, $P < 0.07$), and tended to increase in visceral (Fig. 2E, $P < 0.07$) and subcutaneous adipose tissues (Fig. 2F, $P = 0.1$) of AT2R-

KO vs. WT mice fed a standard diet. HFHF-STZ resulted in increased dietary fatty acid uptake in the heart (Fig. 2A, $P < 0.008$), the liver (Fig. 2B, $P < 0.001$), kidneys (Fig. 2D, $P < 0.002$), visceral (Fig. 2E, $P < 0.001$) and subcutaneous adipose tissues (Fig. 2F, $P < 0.001$) of WT animals. These effects of HFHF-STZ were partially or totally blunted in AT2R-KO mice (Fig. 2A to F). Thus, the AT2R-KO mice exhibited a profile similar to WT fed HFHF.

HFHF-STZ-mediated remodeling of adipose depots is abolished in AT2R-KO mice

Analysis of adipocyte size indicated that a 6-week HFHF-STZ treatment resulted in a significant shift toward larger adipocytes (Fig. 3A, B) and an overall

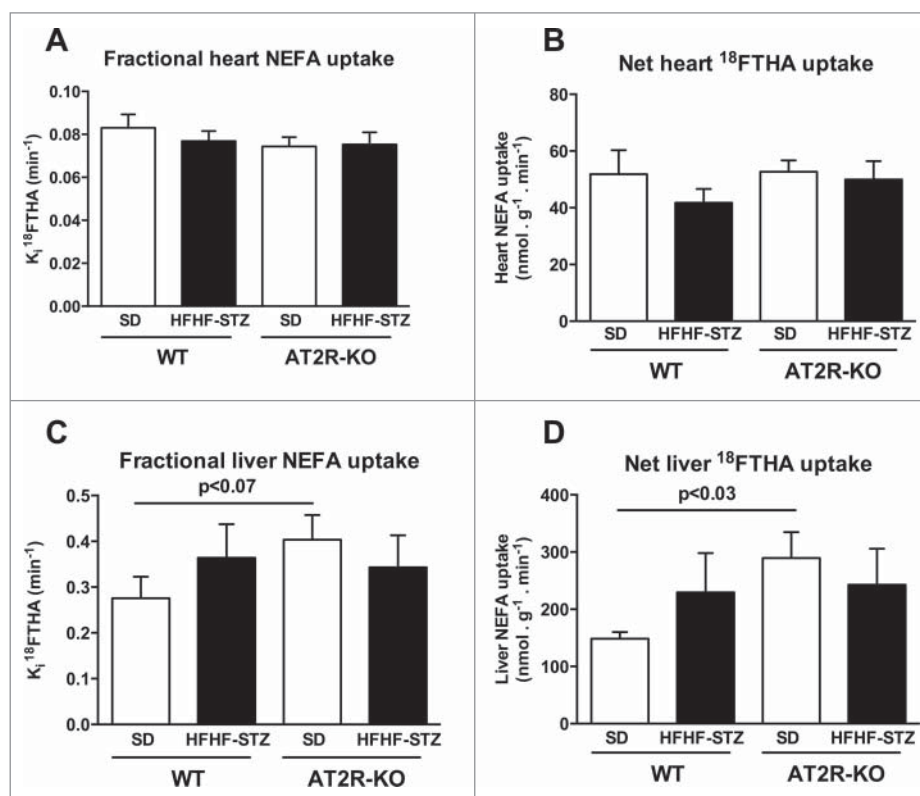


Figure 1. Effect of HFHF-STZ on non-esterified fatty acid uptake of [¹⁸F]-FTHA in WT and AT2R-KO mice. WT and AT2R-KO mice were fed either a standard laboratory rodent diet (SD) or a high-fat/high-fructose diet with small injection of streptozotocin (HFHF-STZ) for 6 weeks. At the end of the experimental period, [¹⁸F]-FTHA was given i.v. during the fasting state. The K_i fractional uptake of [¹⁸F]-FTHA was analyzed by μ PET in the heart (A) and the liver (C); and the K_m net uptake of [¹⁸F]-FTHA was analyzed by μ PET in the heart (B) and the liver (D). Data are presented as mean ± SE (n = 8–10). Statistical analyses of the data were performed using Mann-Whitney test.

increase in mean diameter of adipocytes (Fig. 3C, D), both in subcutaneous and visceral adipose depots in WT mice (Fig. 3A-D). As illustrated in Figure 4, adipocytes of both adipose tissue depots appeared smaller in AT2R-KO animals than WT animals (Fig. 4C vs 4A and 4G vs 4E), both in control and HFHF-STZ mice. Thus, AT2R-KO completely abolished adipocyte remodeling in response to HFHF-STZ (Fig. 4D vs 4B and 4H vs 4F).

Discussion

Over the past decade, considerable evidence confirmed the major role of adipose tissue in the regulation of lean tissue fatty acid exposure. Indeed, the safe storage of lipids in adipose tissue is key to preventing lipotoxicity in non-adipose tissue.^{19,20} Lipotoxicity is characterized by a reduction of glucose transport and utilization in response to excess tissue fatty acid exposure and is considered a

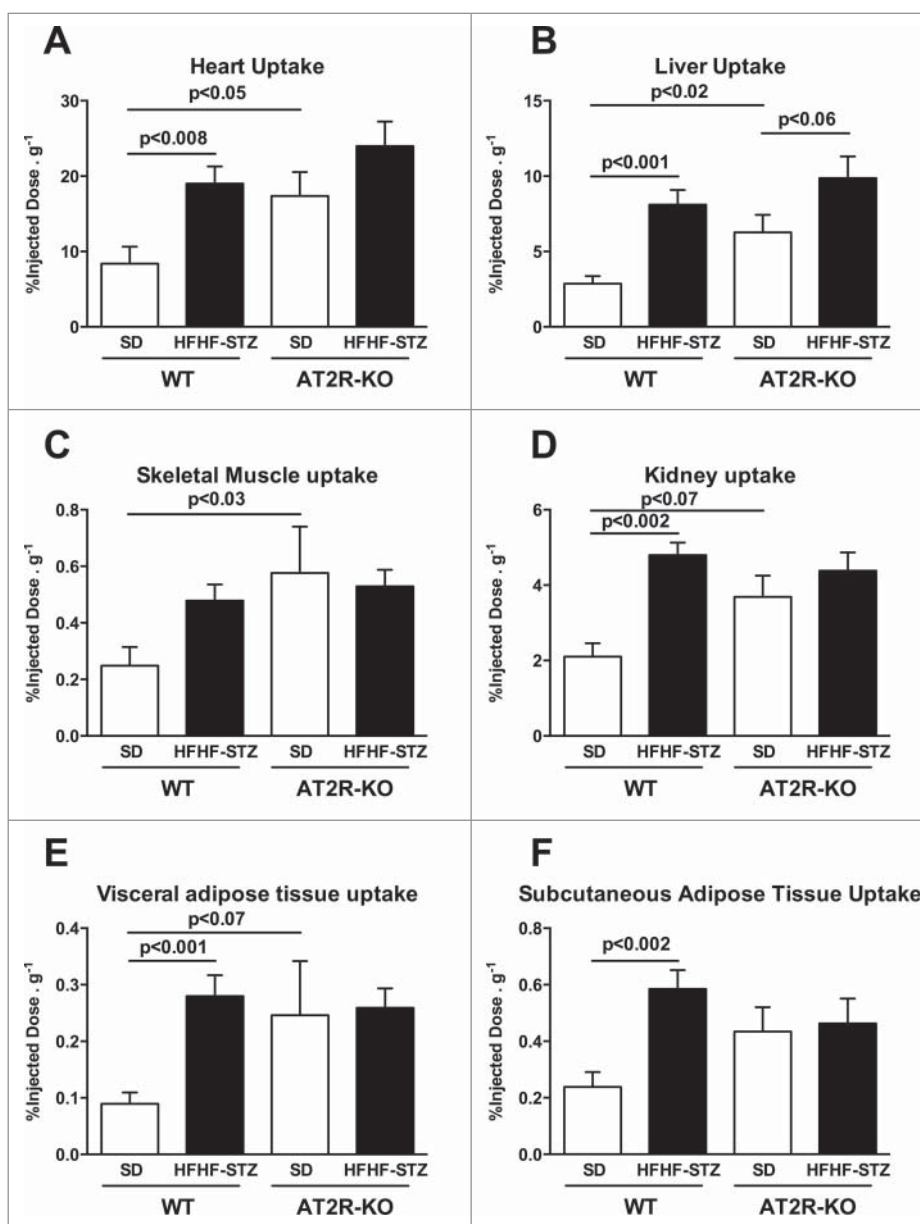


Figure 2. Effect of HFHF-STZ on postprandial dietary fatty acid uptake of [¹⁸F]-FTHA in WT and AT2R-KO mice. WT and AT2R-KO mice were fed either a standard laboratory rodent diet (SD) or a high-fat/high-fructose diet with small injection of streptozotocin (HFHF-STZ) for 6 weeks. At the end of the experimental period, [¹⁸F]-FTHA was given *per os* during the postprandial state. The uptake of [¹⁸F]-FTHA was analyzed in the heart (A), the liver (B), the skeletal muscle (gastrocnemius) (C), the kidney (D), the visceral (retroperitoneal) adipose tissue (E) and the subcutaneous adipose tissue (F). Data are presented as mean ± SE (n = 8–10). Statistical analyses of the data were performed using Mann-Whitney test.

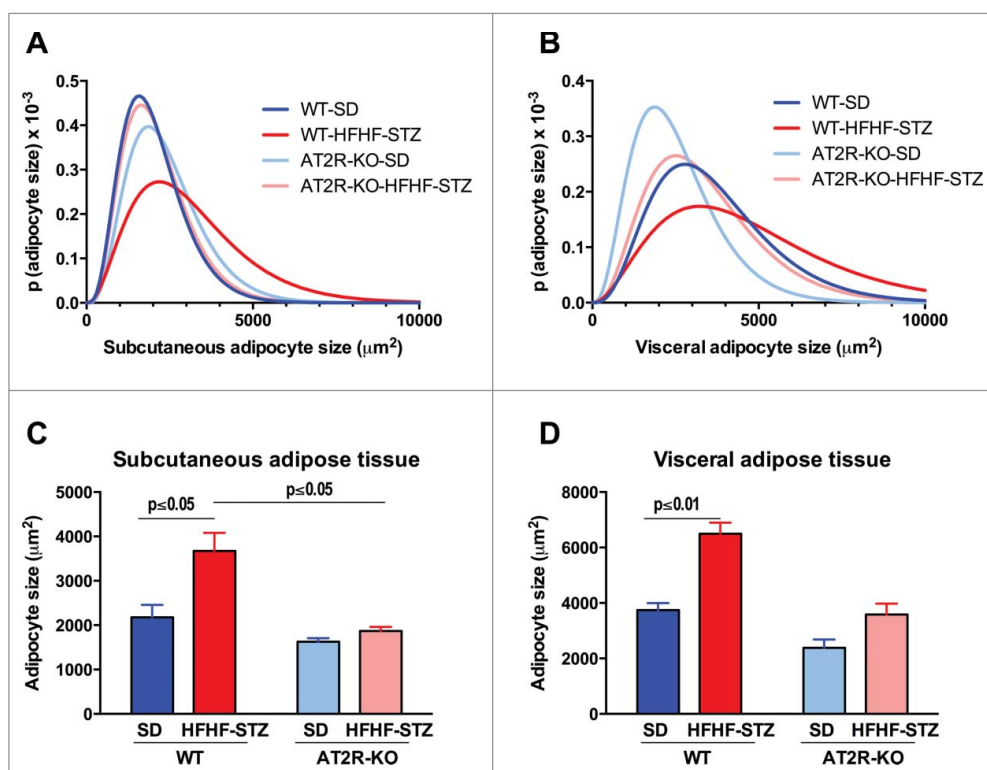


Figure 3. Effect of HFHF-STZ on adipocyte size distribution in WT and AT2R-KO mice. Mice were fed a standard diet (SD) or high-fat/high-fructose diet with STZ (HFHF-STZ) for 6 weeks. Adipocyte size distribution (A, B) and areas (C, D) from subcutaneous adipose tissue (A, C) and visceral (retroperitoneal) (B, D) adipose tissue. Data are presented as mean \pm SE ($n = 8-10$). Statistical analyses were performed using one-way ANOVA followed by the Tukey's multiple comparisons test. (A, C), Statistical significance.

major diabetogenic mechanism effective in animal models and humans. Excess exposure to fatty acids leads to maximal storage of lipids in adipocytes. Such maximal storage capacity (as indicated by the presence of very

large adipocytes) alters adipokine secretion, and activates inflammatory pathways, thereby impairing adipogenesis and initiating insulin resistance.¹⁸ To increase their functionality and prevent the development of insulin

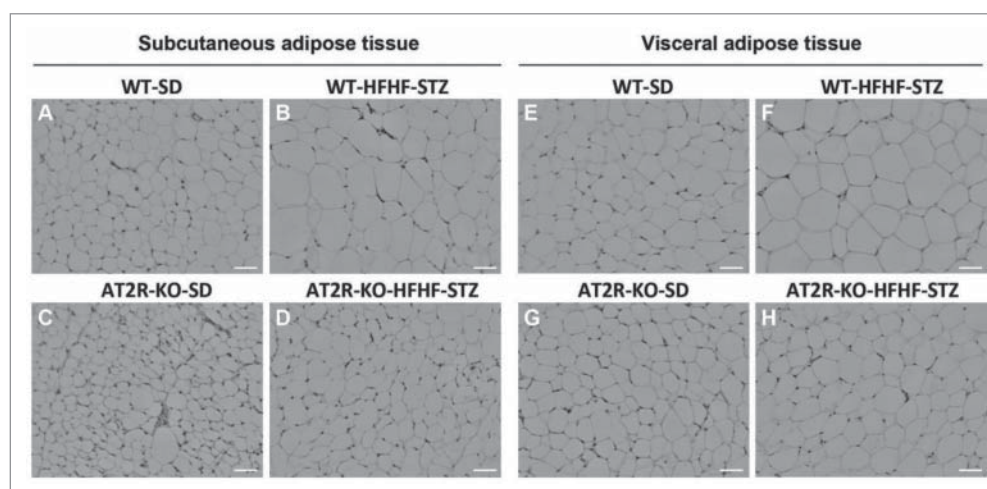


Figure 4. H&E staining of adipose tissue from WT and AT2R-KO mice, after 6 weeks fed a standard diet (SD) or high-fat/high-fructose diet with STZ (HFHF-STZ). Sections ($5 \mu\text{m}$) of subcutaneous (A-D) and visceral (retroperitoneal) adipose tissues (E-H) were stained with H&E. Ten images per histological section were used for analysis. Images were acquired using a Leica microscope equipped with a 10X objective. Scale bar, $40 \mu\text{m}$.

resistance, adipocytes may use 2 strategies, either by increasing the storage capacity of individual adipocytes and/or by recruiting new pre-adipocytes.²⁰ Analyses of adipocyte size indicated that, in the AT2R-KO mice, not only the initial size of adipocytes was smaller compared with the control WT, but the 6-week HFHF-STZ had no effect. These results indicate that the genetic deletion of AT2R abolished HFHF-STZ-induced hypertrophic remodeling of adipocytes. In these conditions, adipose tissue from AT2R-KO mice appears to be resistant to normal expansion following a high-fat diet. These results are in agreement with those of a previous study in which AT2R-KO mice were fed a high-fat diet for 12 weeks.⁷ The authors concluded that AT2R-KO mice are protected against high-fat diet-induced obesity since the deletion of AT2R protected them against adipose tissue hypertrophy and deleterious consequences (such as inflammation and obesity-linked insulin resistance). This interpretation of the data is in accordance with AT2R-KO-mediated blunting of dietary fatty acid spillover induced by HFHF-STZ. On the other hand, detailed morphological examination of adipose tissue has revealed that very small adipocytes in subcutaneous and visceral adipose tissues are associated with impaired adipogenesis,²¹ increased expression of proinflammatory cytokines and decreased expression of genes that regulate adipose tissue fatty acid storage.²² These results thus suggest that the prevalence of very small adipocytes may be implicated in the metabolic dysfunction of white adipose tissues.¹⁸ The small size of adipocytes in the AT2R-KO mice, combined with our results of μ PET, is in agreement with these latter observations and further supports the hypothesis that small adipocytes are unable to increase their size under HFHF-STZ conditions. Indeed, despite the observed increase in NEFA uptake in adipose tissue of AT2R-KO mice, adipocyte size remains small, reflecting an inability to store lipids which might result in the increase in fatty acid uptake in non-adipose tissues such as heart, liver and skeletal muscle that we observed in this study. This conclusion is also consistent with the recent observation that direct AT2R stimulation with the agonist C21/M24 enhances adipocyte differentiation and ameliorates insulin resistance.^{12,23} Using the KK-Ay-type 2 diabetes mice, Ohshima et al.²³ demonstrated that administration of the AT2R agonist, C21/M24,² improved adipocyte dysfunction and restored pancreatic β -cell damage. Interestingly, no variation of visceral adipose tissue weight was found between groups, whereas dietary fatty acid uptake tended to increase, and no variation in adipocyte size was found in AT2R-KO mice fed a standard diet. This could be explained by the increased capacity of the visceral adipose tissue to oxidize fatty acids through an increase of mitochondrial biogenesis.

AT2R has been shown to suppress mitochondrial biogenesis in muscle cells.²⁴ Another explanation would be an increase in fatty acid release from visceral adipose tissue.

When compared to WT mice, the AT2R-KO mice did not display any change in glucose tolerance, circulating NEFA and triglycerides levels, in accordance with the known relative resistance of mice *vs.* rats to diet-induced insulin resistance.²⁵ Nevertheless, AT2R-KO mice had a significant increase in fasting blood glucose and a decrease in plasma insulin levels. Weight gain, food and water intake were also reduced in AT2R-KO mice, an observation which may be explained by increased energy expenditure, whole body lipid oxidation and decreased food intake, as also found by Yvan-Charvet et al.⁷ Ang II is believed to play a major role in water consumption through AT1R activation.²⁶ Nevertheless, AT2R also seems to play an important role in this regulatory pathway. A previous study had shown that water intake is less stimulated by Ang II in AT2R-KO mice.²⁷ AT2R-KO mice fed a control diet showed a decrease in plasma leptin levels, which may be correlated with the decrease in plasma insulin levels.²⁸ On the other hand, HFHF-STZ increased leptin secretion, as found by others,²⁹ in both WT and AT2R-KO mice. The decreased secretion of insulin in AT2R-KO mice fed a control or a HFHF diet could be due to the deleterious action of the AT1R on β -cell survival and insulin biosynthesis and secretion.³⁰ Indeed, some recent publications highlighted the role of AT2R in the regulation of the expression and secretion of insulin by pancreatic islets,^{31,32} demonstrating that activation of AT2R partially ameliorates STZ-induced diabetes in male rats through islet protection.³¹

We found an increase in plasma NEFA uptake in the liver of AT2R-KO mice on the control diet. Ang II plays a role in hepatic fatty acid metabolism by activating hepatic triglyceride production through AT2R activation³³ but AT2R deletion was found to have no effect on genes related to fatty acid oxidation.³⁴ This increase in NEFA uptake by the liver in AT2R-KO mice could be due to the effect of Ang II on AT1R. Indeed, it has been shown that mice that are deficient in AT1R have less hepatic steatosis than WT mice³⁵ and that Ang II induces a pro-fibrotic phenotype in hepatic stellate cells (which only express AT1R³⁶) and thus induces liver fibrosis.³⁷

The heart is a major user of fatty acids derived from circulating triglycerides.¹⁸ Approximately 60 to 70 % of energy is derived from oxidation of fatty acids in the adult heart. Insulin resistant states and type 2 diabetes are associated with increased circulatory NEFA and

triglyceride fluxes.¹⁸ The increase in myocardial uptake of dietary fatty acid in WT mice on HFHF-STZ is consistent with our observations in humans with pre-diabetes, where this increase was found to be associated with early ventricular dysfunction.¹⁰ The increased uptake of dietary fatty acids by the heart of AT2R-KO mice on control diet could be due to an increased activation of AT1R and may thus contribute to the deleterious effect of cardiac AT1R activation observed by others.³⁸

In conclusion, we have shown that adipocyte remodeling occurs before the onset of insulin resistance in the HFHF-STZ mouse model and that AT2R-KO abolishes this early hypertrophic adipocyte remodeling without change in total adiposity. Further studies are needed to determine the molecular mechanisms by which AT2R affects these adaptations to diabetogenic conditions and whether the AT2R could be a relevant target for the prevention of type 2 diabetes.

Materials and methods

Mice, genotyping and experimental protocol

Mice were maintained in a controlled environment with unlimited access to food and water on a 12-h light/dark cycle. All procedures and experiments were approved by the Animal Care and Ethics Committee of the Faculty of Medicine and Health Sciences of the Université de Sherbrooke in accordance with the guidelines of the Canadian Council on Animal Care. Mice hemizygous for targeted disruption of the *Agtr2* gene (AT2R-KO) were generously donated by Prof. Tadashi Inagami (Department of Biochemistry, Nashville University, Nashville, TN, USA).³⁹ AT2R-KO mice on a C57BL/6 genetic background were generated by mating male AT2R-KO mice with female wild-type C57BL/6 mice (Charles River, Montreal, QC, Canada). Because the *Agtr2* gene is on the X chromosome and embryonic stem cells are XY, all F₁ male mice were wild type (WT) and all F₁ females were heterozygous for the mutation. These heterozygous females were mated with F₁ males, giving rise to an F₂ generation that included homozygous females. The hemizygous males were healthy and fertile. RNA from hemizygous males was analyzed by northern blotting to confirm the absence of AT2R transcripts that are normally expressed at high levels in fetuses and in adult brains.³⁹

At 10 weeks of age, male AT2R-KO mice from our colony and WT mice (Charles River, Montreal, QC, Canada) were randomly assigned to either the control or HFHF-treated group and maintained on the following diets for 6 weeks *ad libitum*. Control mice

were fed a standard laboratory diet (Rodent laboratory chow 5001, Purina, St-Louis, MO, USA) and HFHF-treated mice were fed a HFHF diet containing 46.5 % fructose and 25.7 % lard (TD #05482, Teklad Diets, Madison, WI, USA). During the second week of the diet, a single small dose of streptozotocin (STZ, 50 mg.kg⁻¹) (Sigma-Aldrich, Montreal, QC, Canada) was injected intraperitoneally in HFHF-treated mice, whereas control mice were injected with a vehicle (citrate buffer; 1 mL.kg⁻¹).⁸

Glucose tolerance test

At the end of both diets, 8 mice from each group were assessed for glucose tolerance. After a 12-h fasting period, blood glucose (Precision Xtra, Abbott laboratories) was determined before and after (15, 30, 60 and 120 min) an oral administration of dextrose (2 mg per g of animal weight).

Small animal μ PET protocol and tissue collection

All experiments were performed after a 12-h fasting period under anesthesia with 2 % (vol/vol) isoflurane (Abbott Laboratories, Montreal, QC, Canada) delivered through a nose cone. A protocol to determine tissue uptake of plasma NEFA was performed in a first group of animals. Briefly, a catheter was placed into the caudal vein for intravenous injection of 15–20 MBq of [¹⁸F]-FTHA followed by a 40-min dynamic acquisition obtained with the avalanche photodiode-based LabPETTM scanner of the Sherbrooke Molecular Imaging Center (Fig. 5). During imaging, mice rested supine on the scanner bed and were kept warm with a heating pad. A second protocol designed to assess tissue dietary fatty acid uptake was performed in a second set of animals. Briefly, a catheter was placed into a carotid artery for blood sampling and [¹⁸F]-FTHA was given *per os* by gavage mixed in 0.5 mL of Ensure[®]Calorie Plus (Abbott Laboratories, Montreal, QC, Canada) and blood sampling was performed during 2-h.⁸ At the end of experimental procedures, mice were euthanatized by exsanguination and blood samples were collected into EDTA-containing tubes, placed immediately on ice, and plasma was isolated by centrifugation. Plasma insulin, NEFA and triglycerides levels were measured as previously described.⁸ Organs were rapidly collected, washed and counted in a Packard Cobra Gamma Counter to determine the incorporation of [¹⁸F]-FTHA, and fixed in phosphate-buffered 4 % formaldehyde for histology. Results are reported as % ingested dose per g of

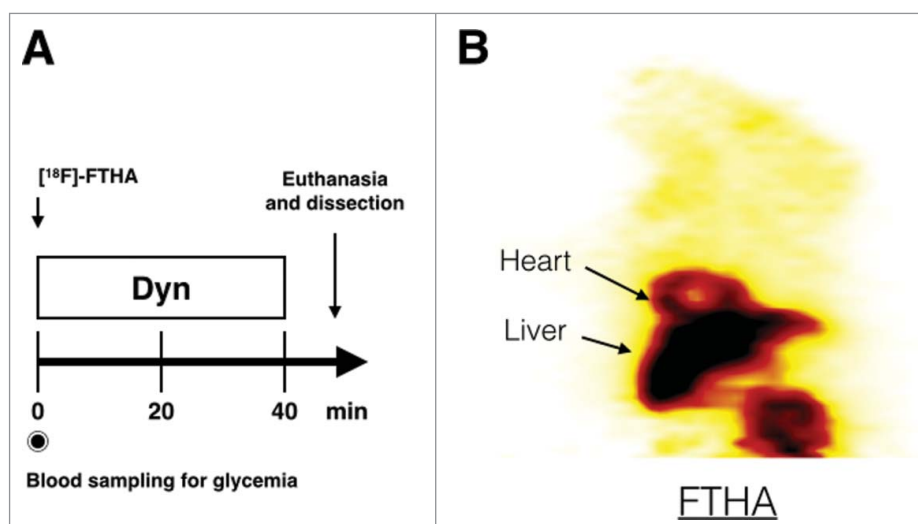


Figure 5. μ TEP protocol. Timeline used to observe intravenous uptake of [18 F]-FTHA in mice (A) and an example of a coronal slice through the μ PET image of FTHA uptake in a WT mouse on a normal diet obtained by this protocol (B). Dyn: Dynamic PET.

tissue.⁸ Retroperitoneal adipose tissue was collected as visceral adipose tissue.

Histology and methodology for measuring adipocyte size in tissues

After fixation, subcutaneous (from the abdominal region) and visceral (from the retroperitoneal region) adipose depots were embedded in paraffin blocks and processed as described previously.¹² Images from hematoxylin–eosin (H&E)-stained slides were acquired with a 20x objective using a Nikon Eclipse TE2000 microscope (Mississauga, ON, Canada) equipped with a CoolSnap fx digital camera (Roper Scientific, Tucson, AZ, USA). Measurement of adipocyte size (as area in μm^2) was performed with a custom-designed software program written using MATLAB (version R2010b; The MathWorks, Inc., Natic, MA, USA). Cell surfaces were used to build a distribution histogram function and the mean \pm SE surface (μm^2) was calculated. Each result represents the sum of 6 to 10 images with 200–500 cells analyzed in each image.¹²

Imaging and statistical analyses

Myocardial and liver plasma NEFA fractional uptake (K_f) and net uptake (K_m) were determined by a Patlak graphical analysis as previously described.⁸ The results are presented as mean \pm SEM of the number of experiments indicated in the text. Statistical analyses of the data were performed using Mann-Whitney test using GraphPad Prism 6.0f for Mac (San Diego, CA, USA). Differences were considered significant for $P \leq 0.05$.

Abbreviations

AT2R	angiotensin II (Ang II) type-2 receptor
AT2R-KO	AT2R-deficient mice
HFHF	high-fat/high-fructose diet
FTHA	14(R,S)-[18 F]-fluoro-6-thia-heptadecanoic acid ([18 F]-FTHA)
NEFA	nonesterified fatty acid
μ PET	micro-positron emission tomography
RAS	renin-angiotensin system
STZ	streptozotocin

Disclosure of potential conflicts of interest

No potential conflicts of interest were disclosed.

Acknowledgment

We thank our technicians Lucie Bouffard, Caroline Mathieu and Stéphanie Larrivée Vanier (from the Division of Endocrinology, Department of Medicine, *Faculté de médecine et des sciences de la santé, Université de Sherbrooke*, Sherbrooke, Quebec, Canada) for their experimental assistance with animal care and treatments and metabolic measurements. We also thank Jean-François Beaudoin and Maxime Paillé (both from the *Sherbrooke Molecular Imaging Center*, Sherbrooke, Quebec, Canada) for their technical assistance with μ TEP. We sincerely thank Prof. Tadashi Inagami (Department of Biochemistry, Nashville University, Nashville, TN, USA) for the gift of the *Agtr2* (AT2R-KO) mice. We are grateful to Dr. Marcel D. Payet (Department of Physiology and Biophysics, *Faculté de médecine et des sciences de la santé, Université de Sherbrooke*, Sherbrooke, Quebec, Canada) for developing the adipocyte morphometric software and Dr. Ouhida Benrezzak for her assistance with all protocols related to animal care and ethics committee. We also thank Margaret Kunach for the English revision of our manuscript. Drs. Nicole Gallo-Payet and André C. Carpentier (CIHR-GSK Chair in Diabetes) are the

guarantors of this work and, as such, had full access to all of the data in the study and take responsibility for the integrity of the data and the accuracy of the data analysis.

Funding

This work was supported by grants from the Canadian Diabetes Association to N.G.-P. and A.C.C., and by the Canada Research Chairs Program to N.G.-P. and by CIHR-GSK Chair in Diabetes to A.C.C. Christophe Noll is the recipient of the *Fonds de Recherche du Québec – Santé* then a CIHR Postdoctoral Fellowship; Sébastien M. Labbé is the recipient of a CIHR Postdoctoral Fellowship. All are members of the FRSQ-funded *Center de recherche clinique du CHUS*.

References

- Steckelings UM, Rompe F, Kaschina E, Namsolleck P, Grzesiak A, Funke-Kaiser H, Bader M, Unger T. The past, present and future of angiotensin II type 2 receptor stimulation. *J Renin Angiotensin Aldosterone Syst* 2010; 11:67-73; PMID:19861348; <http://dx.doi.org/10.1177/1470320309347791>
- Murugiah AMS, Wu X, Wallinder C, Mahalingam AK, Wan Y, Sköld C, Botros M, Guimond M-O, Joshi A, Nyberg F, et al. From the first selective non-peptide AT(2) receptor agonist to structurally related antagonists. *J Med Chem* 2012; 55:2265-78; PMID:22248302; <http://dx.doi.org/10.1021/jm2015099>
- Kaschina E, Grzesiak A, Li J, Foryst-Ludwig A, Timm M, Rompe F, Sommerfeld M, Kemnitz UR, Curato C, Namsolleck P, et al. Angiotensin II type 2 receptor stimulation: a novel option of therapeutic interference with the renin-angiotensin system in myocardial infarction? *Circulation* 2008; 118:2523-32; PMID:19029468; <http://dx.doi.org/10.1161/CIRCULATIONAHA.108.784868>
- Jehle AB, Xu Y, Dimaria JM, French BA, Epstein FH, Berr SS, Roy RJ, Kemp BA, Carey RM, Kramer CM. A nonpeptide angiotensin II type 2 receptor agonist does not attenuate postmyocardial infarction left ventricular remodeling in mice. *J Cardiovasc Pharmacol* 2012; 59:363-8; PMID:22157261; <http://dx.doi.org/10.1097/FJC.0b013e3182444110>
- Iwai M, Tomono Y, Inaba S, Kanno H, Senba I, Mogi M, Horiuchi M. AT2 receptor deficiency attenuates adipocyte differentiation and decreases adipocyte number in atherosclerotic mice. *Am J Hypertens* 2009; 22:784-91; PMID:19444223; <http://dx.doi.org/10.1038/ajh.2009.85>
- Iwai M, Chen R, Li Z, Shiuchi T, Suzuki J, Ide A, Tsuda M, Okumura M, Min L-J, Mogi M, et al. Deletion of angiotensin II type 2 receptor exaggerated atherosclerosis in apolipoprotein E-null mice. *Circulation* 2005; 112:1636-43; PMID:16145000; <http://dx.doi.org/10.1161/CIRCULATIONAHA.104.525550>
- Yvan-Charvet L, Even P, Bloch-Faure M, Guerre-Millo M, Moustaid-Moussa N, Ferre P, Quignard-Boulangue A. Deletion of the angiotensin type 2 receptor (AT2R) reduces adipose cell size and protects from diet-induced obesity and insulin resistance. *Diabetes* 2005; 54:991-9; PMID:15793237; <http://dx.doi.org/10.2337/diabetes.54.4.991>
- Ménard SL, Croteau E, Sarrhini O, Gélinas R, Brassard P, Ouellet R, Bentourkia M, van Lier JE, Rosiers Des C, Lecomte R, et al. Abnormal in vivo myocardial energy substrate uptake in diet-induced type 2 diabetic cardiomyopathy in rats. *Am J Physiol Endocrinol Metab* 2010; 298:E1049-57; <http://dx.doi.org/10.1152/ajpendo.00560.2009>
- Luo J, Quan J, Tsai J, Hobensack CK, Sullivan C, Hector R, Reaven GM. Nongenetic mouse models of non-insulin-dependent diabetes mellitus. *Metab Clin Exp* 1998; 47:663-8; PMID:9627363; [http://dx.doi.org/10.1016/S0026-0495\(98\)90027-0](http://dx.doi.org/10.1016/S0026-0495(98)90027-0)
- Labbe SM, Grenier-Larouche T, Noll C, Phoenix S, Guérin B, Turcotte EE, Carpentier AC. Increased myocardial uptake of dietary Fatty acids linked to cardiac dysfunction in glucose-intolerant humans. *Diabetes* 2012; 61:2701-10; PMID:23093657; <http://dx.doi.org/10.2337/db11-1805>
- Ci X, Frisch F, Lavoie F, Germain P, Lecomte R, van Lier JE, Bénard F, Carpentier AC. The effect of insulin on the intracellular distribution of 14(R,S)-[18F]Fluoro-6-thiaheptadecanoic acid in rats. *Mol Imaging Biol* 2006; 8:237-44; PMID:16791750; <http://dx.doi.org/10.1007/s11307-006-0042-7>
- Shum M, Pinard S, Guimond M-O, Labbé SM, Roberge C, Baillargeon J-P, Langlois M-F, Alterman M, Wallinder C, Hallberg A, et al. Angiotensin II type 2 receptor promotes adipocyte differentiation and restores adipocyte size in high-fat/high-fructose diet-induced insulin resistance in rats. *Am J Physiol Endocrinol Metab* 2013; 304:E197-210; PMID:23149621; <http://dx.doi.org/10.1152/ajpendo.00149.2012>
- Lönn M, Mehlig K, Bengtsson C, Lissner L. Adipocyte size predicts incidence of type 2 diabetes in women. *The FASEB J* 2010; 24:326-31; PMID:19741173; <http://dx.doi.org/10.1096/fj.09-133058>
- Arner P, Arner E, Hammarstedt A, Smith U. Genetic predisposition for Type 2 diabetes, but not for overweight/obesity, is associated with a restricted adipogenesis. *PLoS One* 2011; 6:e18284.
- Nag S, Khan MA, Samuel P, Ali Q, Hussain T. Chronic angiotensin AT2R activation prevents high-fat diet-induced adiposity and obesity in female mice independent of estrogen. *Metab Clin Exp* 2015; 64:814-25; PMID:25869303; <http://dx.doi.org/10.1016/j.metabol.2015.01.019>
- Laurencikiene J, Skurk T, Kulyté A, Hedén P, Aström G, Sjölin E, Rydén M, Hauner H, Arner P. Regulation of lipolysis in small and large fat cells of the same subject. *J Clin Endocrinol Metab* 2011; 96:E2045-9; PMID:21994963; <http://dx.doi.org/10.1210/jc.2011-1702>
- Lewis GF, Carpentier AC, Adeli K, Giacca A. Disordered fat storage and mobilization in the pathogenesis of insulin resistance and type 2 diabetes. *Endocr Rev* 2002; 23:201-29; PMID:11943743; <http://dx.doi.org/10.1210/edrv.23.2.0461>
- Carpentier AC, Labbe SM, Grenier-Larouche T, Noll C. Abnormal dietary fatty acid metabolic partitioning in insulin resistance and Type 2 diabetes. *Clinical Lipidology* 2011; 6:703-16; <http://dx.doi.org/10.2217/clp.11.60>
- de Kloet AD, Krause EG, Woods SC. The renin angiotensin system and the metabolic syndrome. *Physiol Behav* 2010; 100:525-34; PMID:20381510; <http://dx.doi.org/10.1016/j.physbeh.2010.03.018>

20. Virtue S, Vidal-Puig A. Adipose tissue expandability, lipotoxicity and the Metabolic Syndrome—an allostatic perspective. *Biochim Biophys Acta* 2010; 1801:338–49; PMID:20056169
21. McLaughlin T, Sherman A, Tsao P, Gonzalez O, Yee G, Lamendola C, Reaven GM, Cushman SW. Enhanced proportion of small adipose cells in insulin-resistant vs insulin-sensitive obese individuals implicates impaired adipogenesis. *Diabetologia* 2007; 50:1707–15; PMID:17549449; <http://dx.doi.org/10.1007/s00125-007-0708-y>
22. McLaughlin T, Deng A, Yee G, Lamendola C, Reaven G, Tsao P, Cushman SW, Sherman A. Inflammation in subcutaneous adipose tissue: relationship to adipose cell size. *Diabetologia* 2010; 53:369–77; PMID:19816674; <http://dx.doi.org/10.1007/s00125-009-1496-3>
23. Ohshima K, Mogi M, Jing F, Iwanami J, Tsukuda K, Min L-J, Ogimoto A, Dahlöf B, Steckelings UM, Unger T, et al. Direct angiotensin II type 2 receptor stimulation ameliorates insulin resistance in type 2 diabetes mice with PPAR γ activation. *PLoS One* 2012; 7:e48387; PMID:23155382; <http://dx.doi.org/10.1371/journal.pone.0048387>
24. Mitsuishi M, Miyashita K, Muraki A, Itoh H. Angiotensin II reduces mitochondrial content in skeletal muscle and affects glycaemic control. *Diabetes* 2009; 58:710–7; PMID:19074984; <http://dx.doi.org/10.2337/db08-0949>
25. Nagata R, Nishio Y, Sekine O, Nagai Y, Maeno Y, Ugi S, Maegawa H, Kashiwagi A. Single nucleotide polymorphism (–468 Gly to A) at the promoter region of SREBP-1c associates with genetic defect of fructose-induced hepatic lipogenesis [corrected]. *J Biol Chem* 2004; 279:29031–42.
26. Daniels D, Mietlicki EG, Nowak EL, Fluharty SJ. Angiotensin II stimulates water and NaCl intake through separate cell signalling pathways in rats. *Exp Physiol* 2009; 94:130–7; PMID:18723579; <http://dx.doi.org/10.1113/expphysiol.2008.044446>
27. Li Z, Iwai M, Wu L, Shiuchi T, Jinno T, Cui T-X, Horiuchi M. Role of AT2 receptor in the brain in regulation of blood pressure and water intake. *Am J Physiol Heart Circ Physiol* 2003; 284:H116–21; PMID:12388241; <http://dx.doi.org/10.1152/ajpheart.00515.2002>
28. Leroy P, Dessolin S, Villageois P, Moon BC, Friedman JM, Ailhaud G, Dani C. Expression of ob gene in adipose cells. Regulation by insulin. *J Biol Chem* 1996; 271:2365–8; PMID:8576190; <http://dx.doi.org/10.1074/jbc.271.5.2365>
29. Wu T, Qi X, Liu Y, Guo J, Zhu R, Chen W, Zheng X, Yu T. Dietary supplementation with purified mulberry (*Morus australis* Poir) anthocyanins suppresses body weight gain in high-fat diet fed C57BL/6 mice. *Food Chem* 2013; 141:482–7; PMID:23768383; <http://dx.doi.org/10.1016/j.foodchem.2013.03.046>
30. Wang L, Leung PS. The role of renin-angiotensin system in cellular differentiation: implications in pancreatic islet cell development and islet transplantation. *Mol Cell Endocrinol* 2013; 381:261–71; PMID:23994025; <http://dx.doi.org/10.1016/j.mce.2013.08.008>
31. Shao C, Zucker IH, Gao L. Angiotensin type 2 receptor in pancreatic islets of adult rats: a novel insulinotropic mediator. *Am J Physiol Endocrinol Metab* 2013; 305:E1281–91; PMID:24085035; <http://dx.doi.org/10.1152/ajpendo.00286.2013>
32. Shao C, Yu L, Gao L. Activation of Angiotensin Type 2 Receptors Partially Ameliorates Streptozotocin-Induced Diabetes in Male Rats by Islet Protection. *Endocrinology* 2014; 155:793–804; PMID:24302627; <http://dx.doi.org/10.1210/en.2013-1601>
33. Ran J, Hirano T, Adachi M. Angiotensin II infusion increases hepatic triglyceride production via its type 2 receptor in rats. *J Hypertens* 2005; 23:1525–30; PMID:16003179; <http://dx.doi.org/10.1097/01.hjh.0000174077.88121.19>
34. Yvan-Charvet L, Even P, Lamandé N, Ferre P, Quignard-Boulangé A. Prevention of adipose tissue depletion during food deprivation in angiotensin type 2 receptor-deficient mice. *Endocrinology* 2006; 147:5078–86; PMID:16887912; <http://dx.doi.org/10.1210/en.2006-0754>
35. Nabeshima Y, Tazuma S, Kanno K, Hyogo H, Chayama K. Deletion of angiotensin II type I receptor reduces hepatic steatosis. *J Hepatology* 2009; 50:1226–35; <http://dx.doi.org/10.1016/j.jhep.2009.01.018>
36. Bataller R, Ginès P, Nicolás JM, Görbig MN, Garcia-Ramallo E, Gasull X, Bosch J, Arroyo V, Rodés J. Angiotensin II induces contraction and proliferation of human hepatic stellate cells. *Gastroenterology* 2000; 118:1149–56; PMID:10833490; [http://dx.doi.org/10.1016/S0016-5085\(00\)70368-4](http://dx.doi.org/10.1016/S0016-5085(00)70368-4)
37. Kim S-Y, Cho BH, Kim U-H. CD38-mediated Ca²⁺ signaling contributes to angiotensin II-induced activation of hepatic stellate cells: attenuation of hepatic fibrosis by CD38 ablation. *J Biol Chem* 2010; 285:576–82; PMID:19910464; <http://dx.doi.org/10.1074/jbc.M109.076216>
38. Mori J, Zhang L, Oudit GY, Lopaschuk GD. Impact of the renin-angiotensin system on cardiac energy metabolism in heart failure. *J Mol Cell Cardiol* 2013; 63:98–106; PMID:23886814; <http://dx.doi.org/10.1016/j.yjmcc.2013.07.010>
39. Ichiki T, Labosky PA, Shiota C, Okuyama S, Imagawa Y, Fogo A, Niimura F, Ichikawa I, Hogan BL, Inagami T. Effects on blood pressure and exploratory behaviour of mice lacking angiotensin II type-2 receptor. *Nature* 1995; 377:748–50; PMID:7477267; <http://dx.doi.org/10.1038/377748a0>